Journal of Hydrology: Regional Studies 29 (2020) 100686

Contents lists available at ScienceDirect

Journal of Hydrology: Regional Studies

journal homepage: www.elsevier.com/locate/ejrh

Learning from the past – Using palaeoclimate data to better understand and manage drought in South East Queensland (SEQ), Australia

Anthony S. Kiem[a,*], Tessa R. Vance[b], Carly R. Tozer[c], Jason L. Roberts[d], Ramona Dalla Pozza[e], John Vitkovsky[f], Kate Smolders[g], Mark A.J. Curran[d]

[a] Centre for Water, Climate and Land (CWCL), Faculty of Science, University of Newcastle, Callaghan, NSW 2308, Australia
[b] Institute for Marine and Antarctic Studies (Previously Antarctic Climate and Ecosystems Cooperative Research Centre (ACE CRC)), University of Tasmania, Hobart, Tasmania 7004, Australia
[c] CSIRO Oceans and Atmosphere, Hobart, Tasmania, Australia
[d] Australian Antarctic Division, Kingston TAS 7050, Australia
[e] Department of Environment, Land, Water and Planning, Melbourne, Victoria 3000, Australia
[f] Queensland Hydrology, Department of Environment and Science, Dutton Park, Queensland 4102 Australia
[g] Seqwater, Ipswich, Queensland 4305, Australia

ARTICLE INFO

Keywords:
Palaeoclimate
Drought
Hydroclimatic risk
Climate variability
Climate change

ABSTRACT

Study region: South East Queensland (SEQ), Australia.
Study focus: Decision makers in the water sector need to deal with uncertainty about the impacts of climate variability and change. Identifying solutions for hydroclimatic risk adaptation strategies that are both optimal and robust in the presence of this uncertainty presents a difficult challenge. The instrumental hydroclimatic record in Australia is short (~60–120 years depending on location and variable), and fails to encompass enough climate variability to allow the calculation of robust statistics around the baseline risk of extreme events (i.e. multi-year droughts, decadal periods with clustering of major flood events). This paper (i) demonstrates how palaeoclimate data can be used to better understand what is possible with respect to drought frequency and duration in South East Queensland (SEQ), Australia and (ii) investigates some implications from palaeoclimate data for drought planning, drought management and water security decision making.
New hydrological insights for the region: The instrumental period is not representative of the full range of past climate variability. Droughts worse than those in the instrumental record are not only possible, but likely, and the probability of conditions drier than the worst on instrumental record is not zero. This means that current drought risk estimates are at best misleading and probably convey a false sense of security that is not justified given the insights now available from palaeoclimate data.

1. Introduction

Australia is the driest inhabited continent in the world. The Millennium drought (e.g. van Dijk et al., 2013; Kiem et al., 2016)

* Corresponding author.
E-mail address: anthony.kiem@newcastle.edu.au (A.S. Kiem).

https://doi.org/10.1016/j.ejrh.2020.100686
Received 25 February 2020; Received in revised form 20 March 2020; Accepted 23 March 2020
Available online 24 April 2020

affected most of eastern Australia from ~1997–2009 and led to billions of dollars of investment to attempt to secure water supplies (e.g. desalination plants in Melbourne, Sydney and the Gold Coast). Despite these significant investments, we still do not know the true chance of a severe water supply shortage occurring or how reliable existing water supply infrastructure will be in preventing future water shortages. The implications of getting this wrong, and the importance of getting it right, are illustrated by the recent (January 2018) situation in Cape Town, South Africa, where four million people were within three months of running out of water. These uncertainties about existing water security are compounded by the fact that we do not know where, when or how multiyear droughts that typically cause water supply shortages will change in the future (e.g. Sheffield et al., 2012; Van Loon, 2015; Kiem et al., 2016).

Since the 1980s it has been standard practice for water supply agencies to use stochastic models to generate synthetic hydroclimate sequences that preserve the key statistics contained in the observed/instrumental hydroclimate data (usually rainfall, potential evapotranspiration (PET) and streamflow). These synthetic hydroclimate sequences are then input into water supply system simulation models to assess the risk of the supply system storage dropping below key thresholds. The synthetic hydroclimate sequences are also used to develop water supply system operating rules, test different environmental flow strategies, and test and optimise long-term water resource infrastructure plans. While high-quality water supply system simulation models are critically important, their ability to determine water supply risks largely depends on the quality and length of the observed/instrumental hydroclimate data. This is a major limitation in Australia, where observed hydroclimate records are at best only ~120 years long (i.e. from ~1900 to present) but are typically less than ~60 years long. This is a significant problem for Australian water supply agencies that are required to plan for 1-in-1000 to 1-in-10,000 year droughts, because (i) the instrumental records only contain three major droughts – the Federation, World War II, and Millennium droughts (e.g. Verdon-Kidd and Kiem, 2009) and (ii) it is highly likely that past (i.e. pre-1900) droughts were more severe and of substantially longer duration than those observed in the last ~120 years (e.g. Palmer et al., 2015; Vance et al., 2015; Tozer et al., 2016).

In short, we simply do not know how reliable existing water supply systems are. Berghout et al. (2017) recently demonstrated this by showing that relying on short instrumental records leads to significant uncertainty in estimates of current and future water supply system yield and reliability (see Fig. 1). This uncertainty far exceeds the influences of choices made by water managers in the modelling and operation of water supply systems. Importantly, the Berghout et al. (2017) study focussed on a catchment with only moderate year-to-year variability – the uncertainty would be significantly greater for systems with higher year-to-year variability (e.g. catchments in Queensland).

The uncertainties associated with using short instrumental records are compounded because eastern Australia is subject to decadal epochs of enhanced/reduced drought frequency that is strongly related to large-scale ocean-atmosphere circulation patterns such as the El Niño/Southern Oscillation (ENSO) and Interdecadal Pacific Oscillation (IPO) (Power et al., 1999; Kiem and Franks, 2004; Vance et al., 2015). Importantly the probability of water supply shortages are significantly elevated (i.e. 20 times greater) when IPO is positive compared to when IPO is negative (Kiem and Franks, 2004). Despite these insights into physical mechanisms that deliver hydroclimatic extremes to eastern Australia, the practical implications of time-varying risks of extreme climate events (including drought and water supply shortage), and how best to deal with them, are presently unclear (Kiem et al., 2016; Johnson et al., 2016). This is at least partially due to the fact that existing instrumental records do not capture enough cycles of multidecadal variability to give realistic insights into what is plausible.

These realities require a paradigm shift from current practice that assumes probability models calibrated to short instrumental records realistically account for the worst droughts possible and that the chance of water supply shortages does not change over time. These assumptions are clearly incorrect, and leave water supply managers without the tools to properly deal with multidecadal climate variability. Numerous sources of pre-instrumental (palaeoclimate) data (e.g. tree-rings, corals, speleothems and ice cores) have emerged over the last decade (refer to Section 4.2 and the Supplementary Material associated with Kiem et al. (2016) for a detailed review and comparison of existing palaeoclimate information relevant to drought in Australia). These can extend hydroclimatic records by centuries or millennia, which could be of great value to water resources managers and planners.

This study (i) demonstrates how palaeoclimate data can be used to better understand what is possible with respect to drought frequency and duration in SEQ, Australia and (ii) provides recommendations for how insights from palaeoclimate data could be used to improve water security planning and decision making. While other sources of palaeoclimate data exist that could be used to gain insights into pre-instrumental drought frequency and duration in SEQ, our focus is the Law Dome (East Antarctica) (Fig. 1) ice core-based climate proxy because of (i) the absence of local, high resolution palaeoclimate proxies for the study catchments and (ii) the significant relationship between Law Dome summer sea salt concentration record (LD_{SSS}) and rainfall variability in SEQ (Vance et al., 2013, 2015). The LD_{SSS} is derived from chemical analysis of an ice core drilled at Law Dome (Fig. 1). Law Dome has a high annual snowfall rate which produces identifiable layers in the ice core which correspond to annual and seasonal scale climate signals (e.g. Curran et al., 2003; Masson-Delmotte et al., 2003; van Ommen and Morgan, 2010; Vance et al., 2013, 2015). The LD_{SSS}-SEQ rainfall relationship is due to ENSO and IPO being a major influence on interannual variability in Antarctica and the Southern Ocean (Turner, 2004; Schneider et al., 2012; Vance et al., 2013, 2015; Meehl et al., 2019) and SEQ (e.g. Gallant et al., 2012; McMahon and Kiem, 2018). This low to high latitude link that results in coherent signals of southwest Pacific and southern Indian Ocean atmospheric variability being preserved in snowfall deposited on the Antarctic continent (Masson-Delmotte et al., 2003; Vance et al., 2016) also preserves a record of rainfall in eastern Australia (Vance et al., 2013, 2015). The LDsss palaeoclimate proxy is also used because it is annually resolved, accurately dated and significantly longer than other palaeoclimate proxies (of similar temporal resolution) used in Australia. This makes the LDsss record useful for hydroclimate studies where accurate event timing and high temporal resolution (i.e. annual or seasonal or better) are needed.

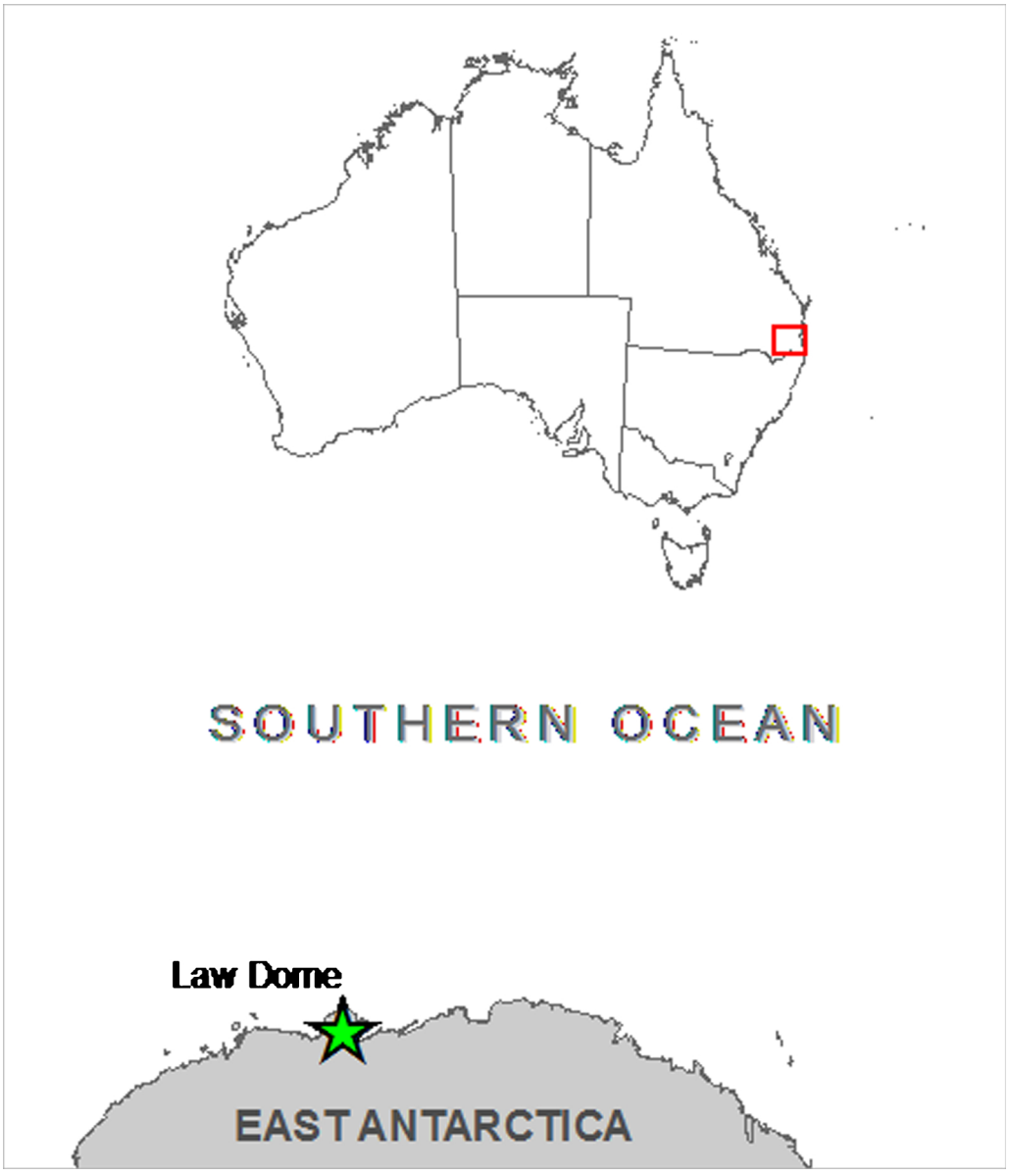

Fig. 1. Location of Law Dome, East Antarctica, in relation to Australia and the South East Queensland (SEQ) study area that is the focus of this paper.

2. Study location and rainfall data

The focus of this study is Lockyer Creek, Stanley River and Upper Brisbane River catchments in SEQ (see Fig. 2). These catchments were identified as important by the relevant decision makers and infrastructure operators (i.e. Seqwater and the Queensland Department of Environment and Science (DES) (which was the Queensland Department of Science, Information Technology and Innovation (DSITI) when this work commenced).

Rainfall data for the study catchments was obtained from high quality (HQ) Australian Bureau of Meteorology (BOM) rainfall gauges in the region and from the Australian Water Availability Project (AWAP, http://www.bom.gov.au/climate/change/about/rain_timeseries.shtml). The AWAP dataset uses topography-resolving analysis methods applied to all available monthly rainfall data passed by a series of internal quality tests to produce gridded monthly rainfall data from 1900 to present at a resolution of approximately 5 km x 5 km (Jones et al., 2009). Both gauged and gridded data are used because (i) HQ rainfall gauge records have minimal missing data and show no spurious trends or inhomogeneity (Lavery et al., 1997) whereas gridded data is known to be associated with biases and uncertainty (e.g. Tozer et al., 2012; King et al., 2013) and ii) the focus is on water security planning which requires understanding of hydrological conditions across catchments (and the wider SEQ region) more so than insights into rainfall variability at individual gauge locations. Hence, given the strengths and weaknesses associated with the two sources of rainfall data

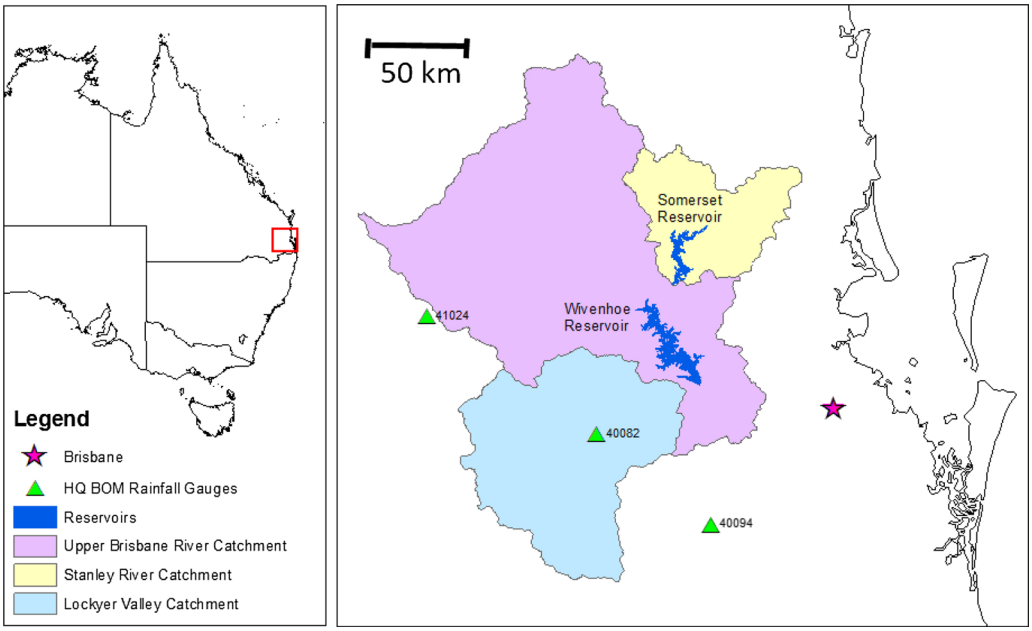

Fig. 2. Location of the catchments investigated in this study. The locations of the high quality (HQ) rainfall gauges used are also shown.

we present results for both.

HQ rainfall gauges with longer records (e.g. ~100 years) are preferred as it enables inclusion of a wider range of climate extremes (wet and dry periods) from the instrumental period and allows better assessment of decadal statistics (e.g. associated with IPO phases). The only suitable HQ gauge within the selected catchments is Gatton (40,082) but two other HQ gauges were found in adjacent catchments and these were also used for some parts of the analysis (see Table 1 for further information about the selected HQ gauges). All three gauges had no missing data between the commencement of observations and 2012 (where 2012 is the end of the study period).

Table 1
Details of high quality (HQ) gauged rainfall data used in this study (Source: Australian Bureau of Meteorology (BOM)).

Gauge Name (Number)	Start	Elevation (m)
Gatton (40082)	Jan 1899	89
Harrisville PO (40094)	Jan 1897	58
Doctors Creek (41024)	Jan 1906	612

3. Methodology used to reconstruct pre-instrumental rainfall for study locations and catchments

In Australia, and many other places around the world, short instrumental climate records (~120 years at best), which are currently used to develop catchment management plans and design water infrastructure, do not capture the full range of climate variability that is possible (e.g. Palmer et al., 2015; Vance et al., 2015; Tozer et al., 2016). Hence, there is a clear need to incorporate palaeoclimate information into water security planning and decision making. However, in Australia there is a dearth of in situ high resolution (i.e. annual or seasonal temporal scale) palaeoclimate records, particularly in catchments that are critical for water supply to key urban areas. One option to deal with this issue is to use remote palaeoclimate proxies that have a teleconnection with the catchment of interest. This means that there is a mechanistic link between the target catchment's climate and the climate at the location of the proxy. As explained in the Introduction, for this study the remote palaeoclimate proxy used is the LD_{SSS} (Vance et al., 2013, 2015).

The methodology used to develop the rainfall reconstructions from the LD_{SSS} record is summarised below:

- The Pearson correlations between annual rainfall (calculated for different 12-month aggregation periods) and LD_{SSS} were

calculated for the HQ gauges listed in Table 1. Non-linear approaches were also tested (e.g. log transform, cube root transform) and no major differences or improvements in the relationship between annual rainfall and LD_{SSS} were found – hence the reconstructions shown in this paper are based on a linear regression model.

- Pearson correlations between rainfall and LD_{SSS} were also calculated for time subsets based on different IPO phases to assess the stationarity and decadal variability of the relationship. The instrumental IPO index is as described in Parker et al. (2007). The IPO index is stratified into phases according to a threshold of +/-0.5 where an index value greater than 0.5 (less than -0.5) is indicative of a positive (negative) phase (Power et al., 1999; Kiem et al., 2003). Following this definition IPO positive phases are 1924 – 1941 and 1979 – 1997 while 1947 – 1975 is IPO negative. Additionally, we assessed IPO phases given in Meehl et al. (2016) which correspond to 1910 – 1941 and 1971 – 1995 (positive) and 1941 – 1971 and 1995 – 2013 (negative).
- The 12-month aggregation period that provided the highest correlation between rainfall recorded at the HQ gauges and LD_{SSS} was selected.
- 1013-year rainfall records were then reconstructed for each HQ gauge and each AWAP grid within each study catchment by rescaling the LD_{SSS} record to match the median and interquartile range of the relevant gauged/gridded data (refer to Tozer et al. (2016) for further details on the rescaling approach).
- 1013-year catchment average rainfall reconstructions were then calculated by averaging the data for the AWAP grids within each of the study catchments.

4. Results

4.1. Rainfall reconstructions for the study gauges and catchments

Table 2 shows the Pearson correlation values between LD_{SSS} and rainfall totals recorded at the selected HQ gauges for the January-December, May-April and July-June 12-month periods for the whole period that HQ gauge and LD_{SSS} data was available and also for different phases of IPO. Three different 12-month aggregation periods are considered because January-December aggregated rainfall was used in the Vance et al. (2013) analysis, May-April is the water year used by Klingaman et al. (2013) in their assessment of rainfall variability in Queensland, and July-June is the traditional water year used for hydrological studies in the SEQ region. The results show that, the January-December year is the 12-month aggregation most often associated with the strongest correlation, followed by May-April and July-June. As such, rainfall reconstructions were developed using statistics from January-December aggregated rainfall.

Table 2
Pearson correlations between LD_{SSS} and "annual" rainfall totals (for different 12-month periods) recorded at HQ gauges within the study region. Bold font indicates correlations that are statistically significant at the 5% level. IPO phases are based on Power et al. (1999).

40082 - Gatton	Jan-Dec (rain leads LD_{SSS} by 11 months)	May-Apr (rain leads LD_{SSS} by 7 months)	Jul-Jun (rain leads LD_{SSS} by 5 months)
1900-2012	**0.26 (0.08;0.42)**	**0.25 (0.06;0.41)**	0.16 (-0.03;0.33)
IPO pos 1 (1924-1941)	**0.63 (0.23;0.85)**	0.24 (-0.26;0.63)	0.14 (-0.35;0.57)
IPO pos 2 (1979-1997)	0.31 (-0.17;0.67)	0.41 (-0.05;0.73)	0.17 (-0.31;0.58)
IPO pos combined	**0.41 (0.09; 0.64)**	**0.35 (0.03;0.61)**	0.15 (-0.18;0.46)
IPO neg (1947-1975)	-0.05 (-0.41;0.32)	0.04 (-0.34;0.40)	0.12 (-0.26;0.47)
40094 – Harrisville	**Jan-Dec**	**May-Apr**	**Jul-Jun**
1900-2012	0.15 (-0.03;0.33)	**0.19 (0.01;0.37)**	0.07 (-0.12;0.25)
IPO pos 1 (1924-1941)	0.29 (-0.20;0.67)	-0.13 (-0.56;0.36)	-0.25 (-0.64;0.25)
IPO pos 2 (1979-1997)	0.36 (-0.12;0.70)	**0.48 (0.04;0.77)**	0.19 (-0.29;0.59)
IPO pos combined	0.31 (-0.02;0.58)	0.25 (-0.08;0.53)	0.02 (-0.31;0.34)
IPO neg (1947-1975)	0.02 (-0.35;0.39)	0.06 (-0.32;0.42)	0.09 (-0.29;0.44)
41024 (Doctors Creek)	**Jan-Dec**	**May-Apr**	**Jul-Jun**
1906-2012	**0.35 (0.17;0.50)**	**0.32 (0.13;0.48)**	**0.23 (0.05;0.41)**
IPO pos 1 (1924-1941)	**0.71 (0.36;0.88)**	0.10 (-0.39;0.54)	0.22 (-0.27;0.63)
IPO pos 2 (1979-1997)	0.32 (-0.16;0.67)	0.36 (-0.11;0.70)	0.22 (-0.26;0.61)
IPO pos combined	**0.43 (0.13;0.66)**	0.29 (-0.04;0.56)	0.21 (-0.12;0.50)
IPO neg (1947-1975)	0.22 (-0.16;0.54)	0.20 (-0.18;0.53)	0.18 (-0.20;0.51)

Table 3
Pearson correlations between LD_{SSS} and annual (Jan-Dec) AWAP catchment average rainfall for selected catchments. Bold font indicates correlations that are statistically significant at the 5% level. IPO phases are based on both Power et al. (1999) and Meehl et al. (2016).

	Lockyer Valley Catchment	Stanley River Catchment	Upper Brisbane River Catchment
1900-2012	**0.27 (0.09;0.44)**	**0.29 (0.11;0.45)**	**0.29 (0.11;0.45)**
Threshold 0.5 (Power et al. (1999)			
IPO pos 1 (1924-1941)	**0.66 (0.28;0.86)**	**0.61 (0.20;0.84)**	**0.60 (0.18;0.83)**
IPO pos 2 (1979-1997)	0.29 (-0.19;0.66)	**0.59 (0.18;0.82)**	0.44 (-0.01;0.75)
IPO pos combined	**0.41 (0.09;0.64)**	**0.59 (0.33;0.77)**	**0.50 (0.22;0.71)**
IPO neg (1947-1975)	0.05 (-0.32;0.41)	-0.06 (-0.42;0.31)	0.04 (-0.33;0.40)
Meehl et al. (2016)			
IPO pos 1 (1910-1941)	**0.60 (0.32;0.78)**	**0.56 (0.27;0.76)**	**0.58 (0.29;0.77)**
IPO neg 1 (1941-1971)	0.02 (-0.34;0.37)	-0.04 (-0.39;0.32)	0.02 (-0.34;0.37)
IPO pos 2 (1971-1995)	**0.43 (0.04;0.70)**	**0.49 (0.12;0.74)**	**0.50 (0.14;0.75)**
IPO neg 2 (1995-2013)	0.05 (-0.43;0.51)	0.12 (-0.37;0.56)	0.07 (-0.41;0.52)
IPO pos combined	**0.47 (0.24;0.65)**	**0.51 (0.29;0.68)**	**0.51 (0.29;0.68)**

Pearson correlation values between LD_{SSS} and January-December AWAP catchment average rainfall for the three selected catchments are provided in Table 3 for the whole period that AWAP and LD_{SSS} data was available (1900 – 2012) and also for different phases of IPO (defined according to both Power et al. (1999) and Meehl et al. (2016)). Fig. 3 shows the spatial correlation between January-December AWAP rainfall and LD_{SSS} across the three selected catchments.

Fig. 3a shows that, according to Mudelsee bootstrapping method (Mudelsee, 2003), correlations between LD_{SSS} and January-December AWAP rainfall are statistically significant at the 5% level for all three study catchments. Also, Table 2 and Table 3 show that, as previously reported in Vance et al. (2013), there is IPO-related non-stationarity in the relationship between rainfall and LD_{SSS}. The SEQ rainfall-LD_{SSS} correlation is stronger in IPO positive phases than it is in IPO negative phases. This is also evident in Fig. 4 which shows the running 13-year correlation between annual (January-December) rainfall recorded at each HQ gauge and LD_{SSS} (Fig. 5 shows the same for AWAP catchment average rainfall and LD_{SSS}). In both Figs. 4 and 5 correlations clearly increase in the positive IPO phases and decrease when the IPO is negative. Vance et al. (2015, 2016) showed that the southern Indian Ocean is typically in a meridional (i.e. north-south) pressure pattern in IPO positive phases relative to a more zonal pattern (west-east) in IPO negative phases and it is thought that this meridional pattern enhances the link between Australia and Law Dome, which explains the stronger relationship in IPO positive phases. The dynamics underlying the decadal shift from meridional to zonal patterns in the mid-latitudes south of Australia that produces this enhanced preservation of subtropical climate signals in the snowfall of East Antarctica is an area of active research. It may be related to synergies between ENSO phase and the Southern Annular Mode (e.g. Fogt et al., 2011; L'Heureux and Thompson, 2006), the previously mentioned IPO influence at high southern latitudes (e.g. Meehl et al., 2019) and/or the variability in springtime polar stratospheric-tropospheric coupling (Lim et al., 2018).

The above results show that despite some, apparently IPO-related, non-stationarity, the relationship between LD_{SSS} and January-

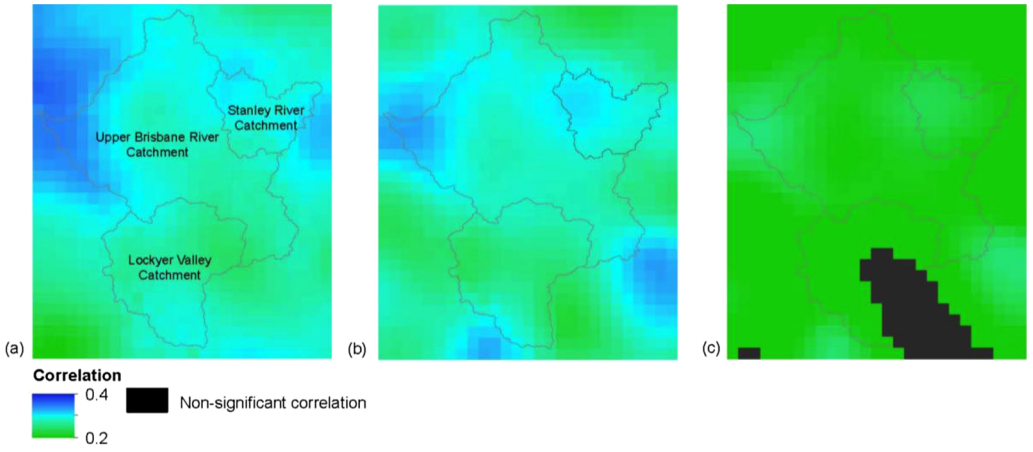

Fig. 3. Correlation between LD_{SSS} and (a) January-December, (b) May-April, (c) July-June AWAP rainfall (1900-2012).

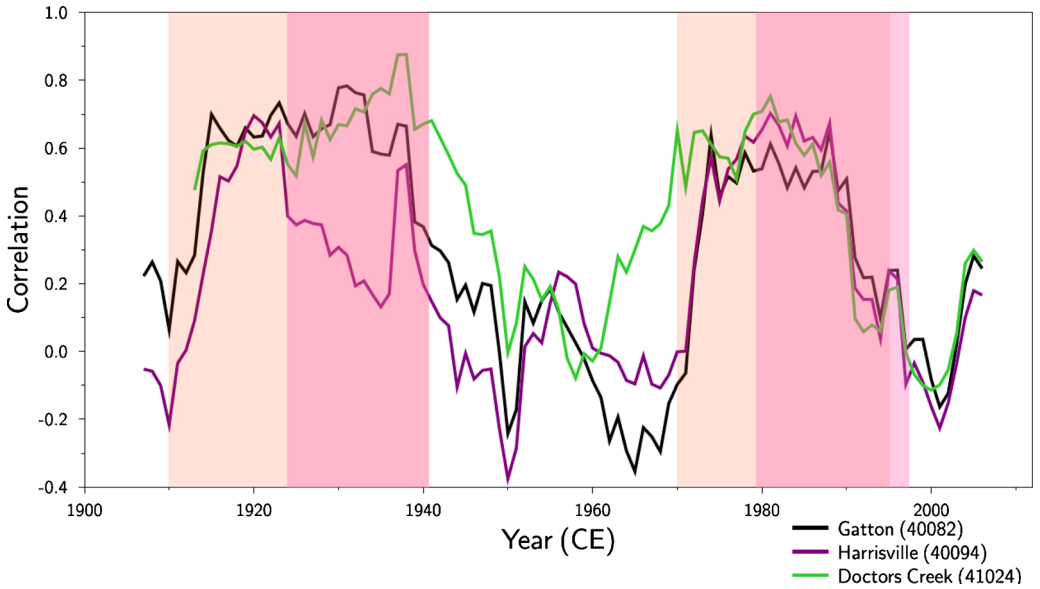

Fig. 4. 13-year running correlation between rainfall recorded at the three HQ gauges used in this study and LD_{SSS}. Red panels indicate IPO positive phases given in Meehl et al. (2016) and pink panels indicate IPO positive phases given in Power et al. (1999). (For interpretation of the references to colour in this figure legend, the reader is referred to the web version of this article).

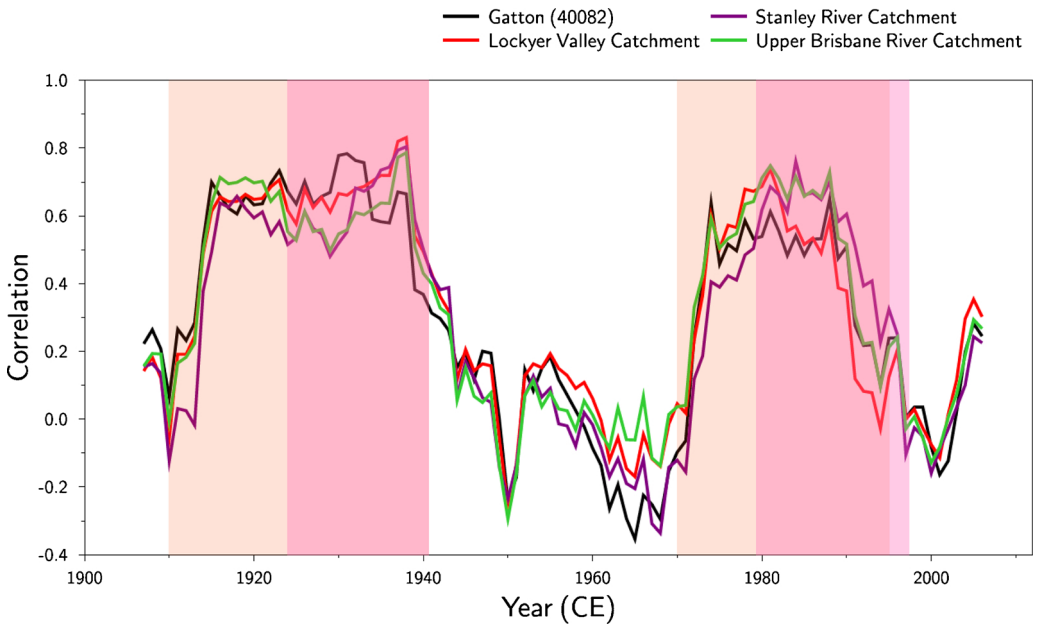

Fig. 5. 13-year running correlation between AWAP catchment average rainfall and rainfall at Gatton (40082) and LD_{SSS}. Red panels indicate IPO positive phases given in Meehl et al. (2016) and pink panels indicate IPO positive phases given in Power et al. (1999). (For interpretation of the references to colour in this figure legend, the reader is referred to the web version of this article).

December rainfall totals in the study catchments is statistically significant across the whole instrumental period. Therefore, the LD_{SSS} record was used to produce 1000 – 2012 (1013-year) annual (January-December) reconstructions for rainfall at Gatton (40082) and catchment average rainfall for the three study catchments (following the process summarised in Section 3). The annual and 10-year smoothed reconstructions for Gatton (40082) are shown in Fig. 6. Fig. 6 also highlights some dry and wet epochs present in the Gatton (40082) rainfall reconstruction. Only Gatton (40082) is shown because the dry/wet epochs are similar for the other HQ gauges and for the three study catchments.

4.2. Pre-instrumental drought frequency and duration

From Fig. 6 it is clear that while the instrumental period (post-1900s period) is relatively dry there are other periods that are as dry or drier for just as long or longer (e.g. the ~1100 – 1250 period). In addition, long wet periods are also evident (e.g. ~1400 – 1650 and ~1750 – 1900).

Table 4 shows the dry epochs in the 1013-year Gatton (40082) annual (January-December) rainfall reconstruction (based on years below the 1900 – 2012 mean). The instrumental period (1900 – 2012) is used as the reference period as this is what is currently used

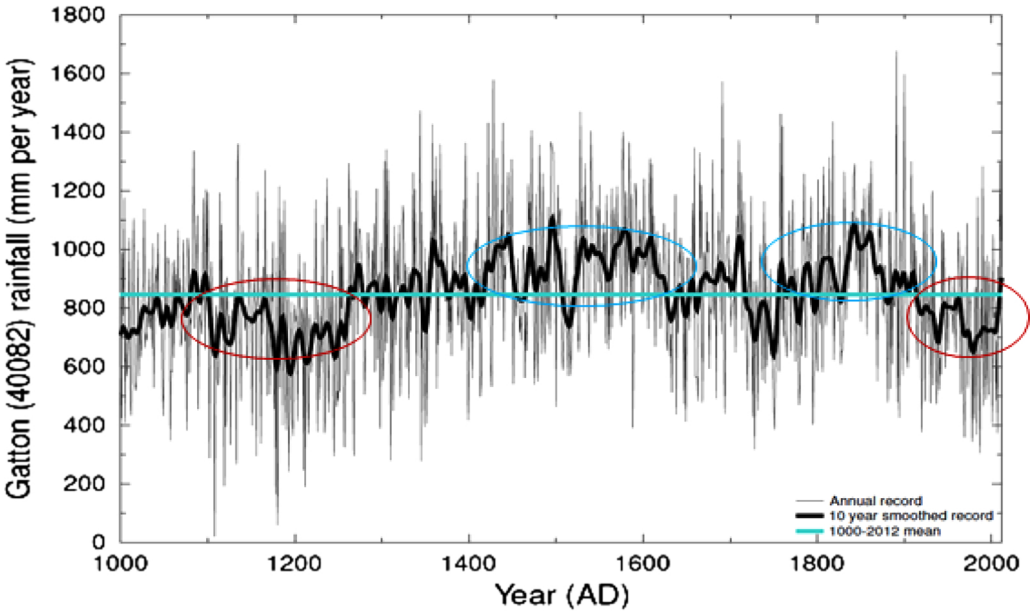

Fig. 6. 1013-year reconstructed annual (January-December) and 10-year Gaussian smoothed rainfall for Gatton (40082) HQ gauge. Multidecadal wet (blue circles) and dry (red circles) periods are indicated. (For interpretation of the references to colour in this figure legend, the reader is referred to the web version of this article).

Table 4
Identification of dry epochs for Gatton (40082) HQ gauge for a) years below mean and b) years defined as per Eq. 1. Mean (773.7 mm) and standard deviation (193.8 mm) calculated over the 1900-2012 instrumental period. Only epochs with four or more consecutive 'dry' years are listed.

a. Dry Epoch defined as < mean rainfall	b. Dry Epoch defined as per Equation 1	
1000 – 1100 (1000s)		
1005 – 1009 (5), 1016 – 1019 (4), 1028 – 1032 (5), 1044 – 1050 (7), 1089 – 1093 (5)	1005 – 1009 (5), 1016 – 1019 (4), 1021 – 1026 (6), 1028 – 1032 (5), 1044 – 1050 (7)	1067 – 1071 (5), 1073 – 1076 (4), 1079 – 1082 (4), 1089 – 1093 (5)
1100 – 1200 (1100s)		
1105 – 1113 (9), 1123 – 1130 (8), 1141 – 1146 (6), 1193 – 1204 (12)	1105 – 1113 (9), 1117 – 1133 (17), 1141 – 1146 (6), 1149 – 1156 (8)	1159 – 1163 (5), 1167 – 1174 (8), 1189 – 1204 (16)
1200 – 1300 (1200s)		
1206 – 1210 (5), 1215 – 1223 (9), 1225 – 1231 (7), 1256 – 1261 (6), 1278 – 1282 (5)	1206 – 1210 (5), 1212 – 1223 (12), 1225 – 1231 (7), 1238 – 1242 (5)	1244 – 1250 (7), 1256 – 1261 (6), 1277 – 1283 (7), 1295 – 1298 (4)
1300 – 1400 (1300s)		
1309 – 1313 (5), 1399 – 1402 (4)	1308 – 1313 (6), 1331 – 1334 (4), 1339 – 1342 (4), 1371 – 1374 (4)	1376 – 1380 (5), 1386 – 1389 (4), 1398 – 1406 (9)
1400 – 1500 (1400s)		
1464 – 1467 (4)	1451 – 1455 (5), 1457 – 1461 (5)	1464 – 1467 (4), 1473 – 1476 (4)
1500 – 1600 (1500s)		
1516 – 1519 (4)	1506 – 1510 (5), 1512 – 1521 (10)	1536 – 1539 (4)
1600 – 1700 (1600s)		
1631 – 1635 (5), 1647 – 1650 (4), 1660 – 1664 (5)	1630 – 1635 (6), 1647 – 1650 (4), 1660 – 1664 (5)	
1700 – 1800 (1700s)		
1701 – 1704 (4), 1742 – 1745 (4), 1747 – 1753 (7), 1763 – 1766 (4)	1701 – 1704 (4), 1717 – 1721 (5), 1725 – 1733 (9), 1742 – 1745 (4)	1747 – 1756 (10), 1761 – 1766 (6), 1778 – 1782 (5), 1794 – 1797 (4)
1800 – 1900 (1800s)		
1827 – 1830 (4)	1819 – 1824 (6), 1827 – 1830 (4)	1886 – 1889 (4)
Instrumental period (1900 – 2012)		
1935 – 1938 (4), 1984 – 1987 (4), 2000 – 2007 (8)	1918 – 1923 (6), 1935 – 1938 (4)	1984 – 1987 (4), 2000 – 2007 (8)

in practice. In addition, following the reasoning and sensitivity analysis presented in Section 5.4 of Tozer et al. (2016), we identify 'not wet' periods based on Eq. 1:

$$not\ wet = years\ where\ rainfall < mean + 0.3 \times standard\ deviation \quad (1)$$

Eq. 1 allows identification of epochs that are generally dry even though some years within the epoch may experience slightly above average rainfall but not enough to break a drought (i.e. total annual rainfall only 0.3 standard deviations above average is not considered enough to break a drought).

Note that in Table 4 only epochs with four or more consecutive 'dry' years are listed. This was a decision informed by discussions with industry stakeholders involved in this work but can easily be adjusted (i) depending on what stakeholders consider to be a serious drought (i.e. how many consecutive years without significant rainfall) or (ii) to test a variety of different drought metrics, a range of drought durations, and/or different operational plans.

The key findings from Table 4 are:

- Some centuries are drier than others (e.g. there are few dry periods in the 1400s, 1500s and 1800s relative to the 1000s, 1100s, 1200s and 1700s).
- Although long dry periods are evident in the instrumental period, they are not unprecedented and the longest dry period in the instrumental record (8 years from 2000 − 2007) has actually been matched or exceeded several times prior to 1900.

In addition to the drought epochs shown in Table 4, drought epochs were also identified for Gatton (40082) HQ gauge based on the methods presented in Biondi et al. (2005, 2008). This involves defining drought epochs relative to above/below median rainfall and then ranking the drought epochs depending on their duration and intensity (total rain during the epoch divided by duration) (Table 5) or their duration, intensity and peak, where peak is the lowest annual rainfall during the drought (Table 6). Again the results show that the 1100 − 1200s dominate the dry periods. Also evident is that varying dry epoch definitions result in different rankings but irrespective of the way you define drought the instrumental record only includes three of the worst 10 droughts in the last 1000 years and the worst drought that has occurred in the instrumental record (1968–1971) is not in the worst five from the last 1000 years.

Table 5
Worst 10 drought epochs at Gatton (40082) HQ gauge over the 1000-2012 reconstruction period. Drought ranking based on drought duration and intensity (total rain during the epoch divided by duration).

Epoch Start Year	Epoch End Year	Duration (Years)	Intensity (mm/year)	Peak (mm)	Score*
1193	1204	12	590.2	238.8	392
1256	1261	6	580.1	322.0	385
1747	1753	7	591.9	382.9	382
1105	1113	9	609.6	15.1	381
1660	1664	5	596.7	481.1	369
1176	1178	3	436.8	161.8	364
1968	1971	4	565.6	356.8	363
1005	1009	5	612.3	405.3	362
1935	1942	8	638.3	471.2	360
2003	2007	5	620.0	370.5	358

* Score is the sum of the ranks (i.e. periods are individually ranked in descending order for duration and intensity and then aggregated so the higher the score the worse the drought).

Table 6
Worst 10 drought epochs at Gatton (40082) HQ gauge over the 1000-2012 reconstruction period. Drought ranking based on drought duration, intensity (total rain during the epoch divided by duration) and peak (lowest annual rainfall during the drought).

Epoch Start Year	Epoch End Year	Duration (Years)	Intensity (mm/year)	Peak (mm)	Score*
1193	1204	12	590.2	238.8	610
1105	1113	9	609.6	15.1	604
1256	1261	6	580.1	322.0	592
1176	1178	3	436.8	161.8	585
1747	1753	7	591.9	382.9	575
1968	1971	4	565.6	356.8	565
1244	1246	3	507.6	291.0	563
1973	1981	9	646.1	340.7	558
2003	2007	5	620.0	370.5	556
1057	1059	3	504.7	345.7	556

* Score is the sum of the ranks (i.e. periods are individually ranked in descending order for duration, intensity and peak and then aggregated so the higher the score the worse the drought).

Table 7
Comparison of important statistics obtained from the instrumental (1900-2012) record of annual (Jan-Dec) rainfall and the 1000-2012 reconstruction of annual (Jan-Dec) rainfall for the Gatton (40082) HQ gauge.

Statistic	Instrumental (1900 – 2012)	Reconstruction (1000 – 2012)
Mean	773.7	848.5
Standard deviation	193.8	247.8
Maximum	1241.4	1686.4
Minimum	354.5	15.1
Max of the 113 moving averages for 1000 – 2012	773.7	971.9
Min of the 113 moving averages for 1000 – 2012	773.7	702.0
Max of the 113 standard deviations for 1000 – 2012	193.8	278.4
Min of the 113 standard deviations for 1000 – 2012	193.8	201.1
Max consecutive years below mean	8 (2000 – 2007)	12 (1193 – 1204)
Max consecutive years below mean + 0.3*SD	8 (2000 – 2007)	17 (1117 – 1133)
Maximum drought duration (where drought is defined as volume of rain > 20 % below average)	11 (1997 – 2007)	87 (1175 – 1261)
Maximum drought duration (where drought is defined as volume of rain > 30 % below average)	4 (2000 – 2003)	12 (1189 – 1200)
Maximum drought duration (where drought is defined as volume of rain > 40 % below average)	2 (1918/19, 1922/23, 1993/94)	6 (1176 – 1181, 1193 – 1198)

4.3. Comparison of drought statistics calculated using the instrumental record versus the palaeoclimate data

Table 7 compares, for the Gatton (40082) HQ gauge, some important statistics obtained from the instrumental (1900 – 2012) record of annual (Jan-Dec) rainfall and the 1000 – 2012 reconstruction of annual (Jan-Dec) rainfall. It is immediately obvious that for every statistic considered there are substantial differences between the statistics derived from the relatively short instrumental record and the statistics derived from the longer 1000 – 2012 reconstruction. For example, the mean in the 1000 – 2012 reconstruction is 10 % higher than the 1900 – 2012 mean, the standard deviation is 28 % higher, the maximum annual total is 36 % higher, and the minimum annual total is 96 % lower.

Some of these differences are to be expected given the different sample sizes being considered. Therefore, the average and standard deviation for each 113 year period (i.e. equal to the number of years in the 1900 – 2012 instrumental record) in the 1000 – 2012 reconstruction is calculated and compared with the mean and standard deviation from the instrumental (1900 – 2012) period (Fig. 7). Again, it is clear that the instrumental and pre-instrumental statistics are very different. From Table 7, the average in pre-instrumental 113 year periods was between 26 % higher and 9% lower than the average over the instrumental 1900 – 2012 period. Similarly, the standard deviation in pre-instrumental 113 year periods was between 4% and 44 % higher than the standard deviation over the 1900 – 2012 instrumental period. From Fig. 7a, the fact that the instrumental mean is below the box means that at least 75 % of the other 113 year means from 1000 – 2012 are greater than that observed in the instrumental 113 year period. For standard deviation (Fig. 7b) the results are even more glaring, with instrumental standard deviation lower than almost all of the other 113 year standard deviations from 1000 – 2012 (i.e. the standard deviation observed in the instrumental 113 years is a statistical outlier in terms of how low it is). In summary, Table 7 and Fig. 7 again emphasises that the 1900 – 2012 instrumental record underestimates (or at least misrepresents) the full range of rainfall variability that has occurred, and is possible, in SEQ.

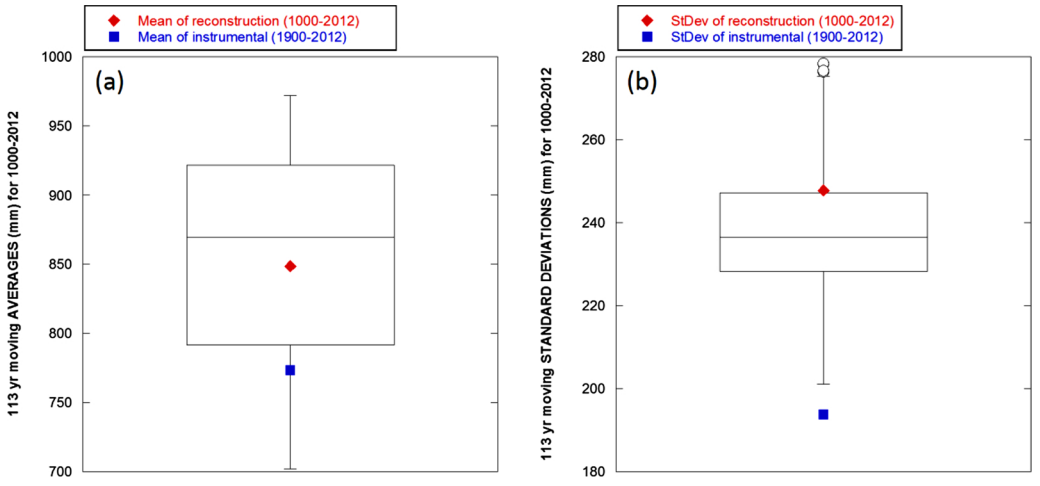

Fig. 7. Distribution of (a) 113 year means and (b) 113 standard deviations obtained from the 1000-2012 reconstruction and compared with the mean and standard deviations from the instrumental (1900-2012) (blue square) and the reconstructed (1000-2012) (red diamond) rainfall for Gatton (40082) HQ gauge. (For interpretation of the references to colour in this figure legend, the reader is referred to the web version of this article).

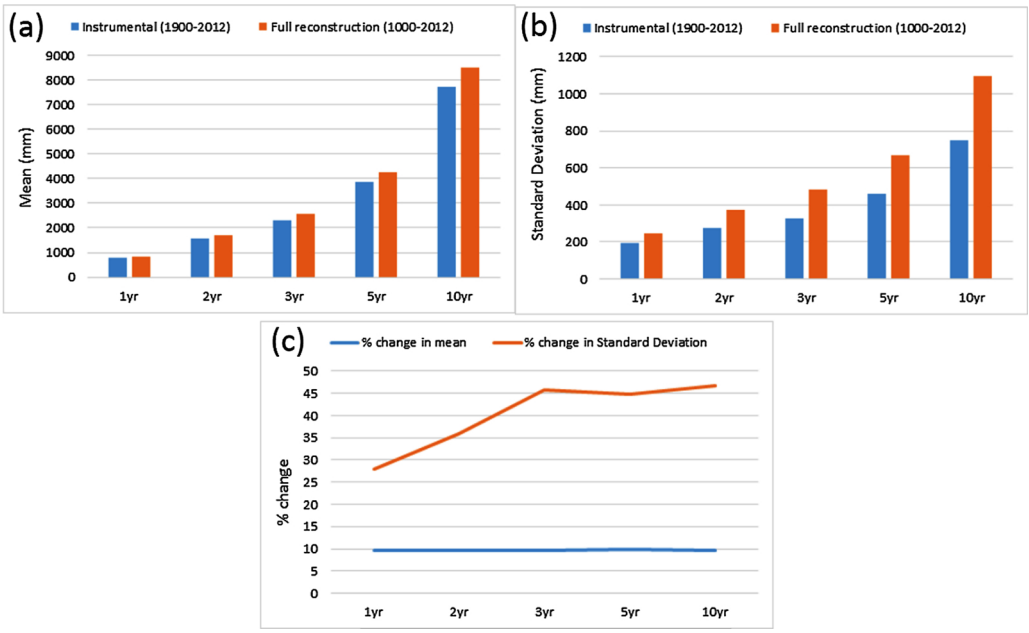

Fig. 8. (a) Mean and (b) standard deviation of 1, 2, 3, 5 and 10 year annual (Jan-Dec) rainfall totals at Gatton (40082) HQ gauge obtained from the instrumental (1900-2012) and reconstructed (1000-2012) records. (c) shows the percentage change in mean and standard deviation when the full reconstruction is compared with the instrumental (i.e. 100 x (reconstructed – instrumental) / reconstructed).

4.4. Implications of palaeoclimate insights for drought planning, drought management and water security decision making

Fig. 8 shows the differences between the instrumental and reconstructed records in another way to indicate how insights from palaeoclimate data might be incorporated in drought planning, drought management and water security decision making. Consistent with the results already presented, Fig. 8 shows that clear differences exist between the mean and standard deviation of 1, 2, 3, 5 and 10 year annual (Jan-Dec) rainfall totals at Gatton (40082) HQ gauge. The mean from the full reconstruction period (1000 – 2012) is ~10 % higher than the 1900 – 2012 mean for all multi-year periods investigated. However, critical for understanding and dealing with drought and other extremes, the reconstructed standard deviation is 28 %, 36 %, 46 %, 45 %, and 48 % higher for 1, 2, 3, 5 and 10 year rainfall totals respectively. These differences would result in markedly different outputs from stochastic climate modelling using the two different inputs (i.e. instrumental and reconstructed). Further, the hydroclimatic risk profiles, robustness and cost-benefit of various water resources planning and adaptation strategies would also be very different if statistics from the 1000 – 2012 reconstructed rainfall were used instead of (or in addition to) the 1900 – 2012 instrumental record.

Fig. 9 uses the multi-year rainfall totals summarised in Fig. 8 to show how estimates for the probability of multi-year droughts of different durations (and different magnitudes) change depending on whether the instrumental (1900 – 2012) or reconstructed (1000 – 2012) annual rainfall from the Gatton (40082) HQ gauge is used. Again, Fig. 9 shows that for all durations and magnitudes the instrumental record misrepresents the probability of drought. Fig. 10, puts this into context by showing that the instrumental record always underestimates the probability of drought. In other words, irrespective of the multi-year period or drought magnitude being investigated the probability is always higher when the reconstruction record is used, demonstrating again that the instrumental record does not properly capture the full range of variability that has occurred or is possible. Also important to note is that, according

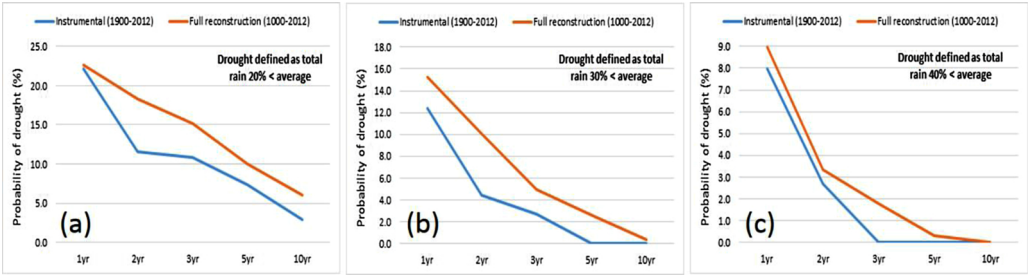

Fig. 9. Probability of multi-year droughts of different durations calculated using the instrumental (1900-2012) and reconstructed (1000-2012) annual rainfall from the Gatton (40082) HQ gauge. Drought is defined as a multi-year period where the total volume of rainfall over that period is (a) 20 % less than average, (b) 30 % less than average, (c) 40 % less than average.

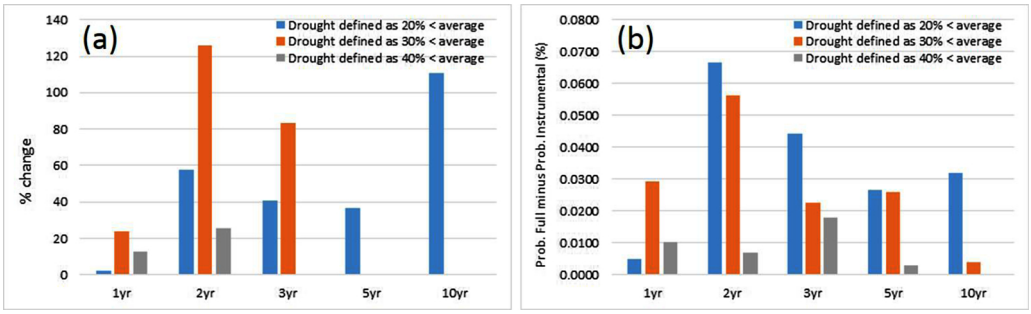

Fig. 10. (a) Percentage difference (100 x (reconstructed – instrumental) / reconstructed) in the probability of multi-year drought when instrumental (1900-2012) and reconstructed (1000-2012) annual rainfall from the Gatton (40082) HQ gauge. (b) As with (a) but absolute differences instead (Full reconstruction minus instrumental).

to the instrumental record, 5- and 10-year periods associated with 30 % less rainfall overall are not possible (i.e. probability = 0) but Fig. 10c shows that these conditions have occurred before and while it is true they are rare (probability of 2.5 % and 0.4 % respectively) the consequences of such events are high. Similar can be said about the 3- and 5-year periods associated with 40 % less rainfall overall. Since risk is a function of likelihood and consequence this means that current drought risk estimates, determined using the instrumental record or using stochastic generation based only on statistics from the instrumental record, are at best misleading and probably convey a false sense of security that is not justified given the insights now available from palaeoclimate data.

5. Conclusions

This study demonstrated how palaeoclimate data can be used to supplement instrumental data to get (i) a better understanding into the range of variability that is possible and (ii) more realistic estimates for the likelihood of multi-year droughts.

The key findings were:

- Some centuries are drier than others (e.g. there are few dry periods in the 1400s, 1500s and 1800s relative to the 1000s, 1100s, 1200s and 1700s).
- The 2000 – 2007 SEQ drought has almost certainly been exceeded many times over the past 1000 years.
- Droughts worse than those seen in the instrumental record are not only possible, but likely.
- The probability of conditions much drier than the worst on instrumental record is not zero.

It is acknowledged that there are uncertainties associated with palaeoclimate data (e.g. Zhang et al., 2018). Some sources of these uncertainties include: non-stationarities in how the climate teleconnections operate when using remote palaeoclimate proxies such as the LDsss used here (e.g. Gallant et al., 2013); dating error prior to the pre-instrumental record which can affect event duration; the potential to over interpret palaeoclimate proxy records that only explain a percentage of the actual variability in any given region; and the temporal resolution of the palaeoclimate proxy. In addition, a limitation of this study is that only one source of palaeoclimate information was used (the LDsss palaeoclimate proxy from Vance et al. (2015)). However, it should be noted that insights about timing and duration of IPO phases and associated dry/wet epochs emerging from the Vance et al. (2015) palaeoclimate proxy have subsequently been verified in other independent studies – one from a low resolution local hydroclimate proxy from the SEQ region (Barr et al., 2019) and an entirely independent tropical Pacific tree ring reconstruction of the IPO (Buckley et al., 2019). These more recent studies add to the multiple lines of evidence, including that presented here, that suggest that the instrumental period is not representative of the full range of past climate variability in SEQ. For every statistic considered the full reconstruction periods (1000 – 2012) gave very different results to that obtained if only the instrumental (1900 – 2012) period is considered. These differences would result in markedly different outputs from stochastic climate modelling using the two different inputs (i.e. instrumental and reconstructed). This means that current drought risk estimates, determined using the instrumental record or using stochastic generation based only on statistics from the instrumental record, are at best misleading and probably convey a false sense of security that is not justified given the insights now available from palaeoclimate data.

Ongoing research that builds on this study is being conducted to collect, develop and compare different palaeoclimate records (remote and local proxies) relevant to hydroclimatic conditions in eastern Australia. Where there is agreement on certain aspects (e.g. timing, duration and frequency of dry epochs) then this information is used to better understand, quantify and manage drought risk. However, disagreements and inconsistencies also exist across the different sources of palaeoclimate information so research is also being conducted to develop approaches that explicitly account for the presence of errors and uncertainties in the palaeoclimate records with the aim being to maximise the practical usefulness of palaeoclimate information for drought planning, drought management and water security decision making.

Author statement

Anthony S. Kiem: conceptualisation, methodology, analysis, writing of original draft and subsequent revisions and finalisation.

Tessa R. Vance: conceptualisation, methodology, collection/development/provision of ice core information used in the rainfall reconstruction, writing of original draft and subsequent revisions and finalisation.

Carly R. Tozer: methodology, analysis, writing – reviewing and editing.

Jason L. Roberts: conceptualisation, methodology, collection/development/provision of ice core information used in the rainfall reconstruction, writing – reviewing and editing.

Ramona Dalla Pozza: conceptualisation from industry/government perspective, supply of hydroclimatic data, identification of study catchments, writing – reviewing and editing.

John Vitkovsky: conceptualisation from industry/government perspective, supply of hydroclimatic data, identification of study catchments, writing – reviewing and editing.

Kate Smolders: conceptualisation from industry/government perspective, supply of hydroclimatic data, identification of study catchments, writing – reviewing and editing.

Mark A. J. Curran: collection/development/provision of ice core information used in the rainfall reconstruction, writing – reviewing and editing.

Declaration of Competing Interest

The authors declare that they have no known competing financial interests or personal relationships that could have appeared to influence the work reported in this paper.

Acknowledgments

The work conducted to produce this paper was funded by:

• Queensland Department of Environment and Science (DES)(which was the Queensland Department of Science, Information Technology and Innovation (DSITI) when this work commenced);

• Seqwater(www.seqwater.com.au/);

• Australian Research Council Discovery Projecton “Flooding in Australia – are we properly prepared for how bad it can get?” (Project number: DP180102522);

• Australian Research Council Special Research Initiative for Antarctic Gateway Partnership(Project number: SR140300001).

References

Barr, C., Tibby, J., Leng, M.J., Tyler, J.J., Henderson, A.C.G., Overpeck, J.T., Simpson, G.L., Cole, J.E., Phipps, S.J., Marshall, J.C., McGregor, G.B., Hua, Q., McRobie, F.H., 2019. Holocene El Niño–Southern Oscillation variability reflected in subtropical Australian precipitation. Sci. Rep. 9 (1), 1627. https://doi.org/10.1038/s41598-019-38626-3.

Berghout, B., Henley, B.J., Kuczera, G., 2017. Impact of hydroclimate parameter uncertainty on system yield. Aust. J. Water Resour. 1–10. https://doi.org/10.1080/13241583.2017.1404550.

Biondi, F., Kozubowski, T.J., Panorska, A.K., 2005. A new model for quantifying climate episodes. Int. J. Climatol. 25 (9), 1253–1264. https://doi.org/10.1002/joc.1186.

Biondi, F., Kozubowski, T.J., Panorska, A.K., Saito, L., 2008. A new stochastic model of episode peak and duration for eco-hydro-climatic applications. Ecol. Modell. 211 (3), 383–395. https://doi.org/10.1016/j.ecolmodel.2007.09.019.

Buckley, B.M., Ummenhofer, C.C., D'Arrigo, R.D., Hansen, K.G., Truong, L.H., Le, C.N., Stahle, D.K., 2019. Interdecadal Pacific Oscillation reconstructed from trans-Pacific tree rings: 1350–2004 CE. Clim. Dyn. 53 (5), 3181–3196. https://doi.org/10.1007/s00382-019-04694-4.

Curran, M.A.J., van Ommen, T.D., Morgan, V.I., Phillips, K.L., Palmer, A.S., 2003. Ice core evidence for Antarctic Sea ice decline since the 1950s. Science 302 (5648), 1203–1206. https://doi.org/10.1126/science.1087888.

Fogt, R.L., Bromwich, D.H., Hines, K.M., 2011. Understanding the SAM influence on the South Pacific ENSO teleconnection. Clim. Dyn. 36 (7), 1555–1576. https://doi.org/10.1007/s00382-010-0905-0.

Gallant, A.J.E., Kiem, A.S., Verdon-Kidd, D.C., Stone, R.C., Karoly, D.J., 2012. Understanding hydroclimate processes in the Murray-Darling Basin for natural resources management. Hydrol. Earth Syst. Sci. 16, 2049–2068. https://doi.org/10.5194/hess-16-2049-2012.

Gallant, A.J.E., Phipps, S.J., Karoly, D.J., Mullan, A.B., Lorrey, A.M., 2013. Nonstationary australasian teleconnections and implications for paleoclimate reconstructions. J. Clim. 26 (22), 8827–8849. https://doi.org/10.1175/jcli-d-12-00338.1.

Johnson, F., White, C.J., van Dijk, A., Ekstrom, M., Evans, J.P., Jakob, D., Kiem, A.S., Leonard, M., Rouillard, A., Westra, S., 2016. Natural hazards in Australia: floods. Clim. Change 139 (1), 21–35. https://doi.org/10.1007/s10584-016-1689-y.

Jones, D.A., Wang, W., Fawcett, R., 2009. High-quality spatial climate data-sets for Australia. Aust. Meteorol. Oceanogr. J. 58, 233–248.

Kiem, A.S., Franks, S.W., 2004. Multi-decadal variability of drought risk - Eastern Australia. Hydrol. Process. 18 (11), 2039–2050. https://doi.org/10.1002/hyp.1460.

Kiem, A.S., Franks, S.W., Kuczera, G., 2003. Multi-decadal variability of flood risk. Geophys. Res. Lett. 30 (2), 1035. https://doi.org/10.1029/2002GL015992.

Kiem, A.S., Johnson, F., Westra, S., van Dijk, A., Evans, J.P., O'Donnell, A., Rouillard, A., Barr, C., Tyler, J., Thyer, M., Jakob, D., Woldemeskel, F., Sivakumar, B., Mehrotra, R., 2016. Natural hazards in Australia: droughts. Clim. Change 139 (1), 37–54. https://doi.org/10.1007/s10584-016-1798-7.

King, A.D., Alexander, L.V., Donat, M.G., 2013. The efficacy of using gridded data to examine extreme rainfall characteristics: a case study for Australia. Int. J. Climatol. 33 (10), 2376–2387. https://doi.org/10.1002/joc.3588.

Klingaman, N.P., Woolnough, S.J., Syktus, J., 2013. On the drivers of inter-annual and decadal rainfall variability in Queensland, Australia. Int. J. Climatol. 33 (10), 2413–2430. https://doi.org/10.1002/joc.3593.

L'Heureux, M.L., Thompson, D.W.J., 2006. Observed relationships between the el niño–Southern oscillation and the extratropical zonal-mean circulation. J. Clim. 19 (2), 276–287. https://doi.org/10.1175/jcli3617.1.

Lavery, B., Joung, G., Nicholls, N., 1997. An extended high-quality historical rainfall dataset for Australia. Austr. Meteorol. Mag. 46, 27–38.

Lim, E.-P., Hendon, H.H., Thompson, D.W.J., 2018. Seasonal evolution of Stratosphere-Troposphere Coupling in the Southern Hemisphere and implications for the

predictability of surface climate. J. Geophys. Res. Atmos. 123 (21), 12. https://doi.org/10.1029/2018jd029321. 002-12,016.
Masson-Delmotte, V., Delmotte, M., Morgan, V., Etheridge, D., van Ommen, T., Tartarin, S., Hoffmann, G., 2003. Recent southern Indian Ocean climate variability inferred from a Law Dome ice core: new insights for the interpretation of coastal Antarctic isotopic records. Clim. Dyn. 21 (2), 153–166. https://doi.org/10.1007/s00382-003-0321-9.
McMahon, G.M., Kiem, A.S., 2018. Large floods in South East Queensland, Australia: is it valid to assume they occur randomly? Aust. J. Water Resour. 22 (1), 4–14. https://doi.org/10.1080/13241583.2018.1446677.
Meehl, G.A., Hu, A., Santer, B.D., Xie, S.-P., 2016. Contribution of the Interdecadal Pacific Oscillation to twentieth-century global surface temperature trends. Nat. Clim. Chang. 6 (11), 1005–1008. https://doi.org/10.1038/nclimate3107.
Meehl, G.A., Arblaster, J.M., Chung, C.T.Y., Holland, M.M., DuVivier, A., Thompson, L., Yang, D., Bitz, C.M., 2019. Sustained ocean changes contributed to sudden Antarctic sea ice retreat in late 2016. Nat. Commun. 10 (1), 14. https://doi.org/10.1038/s41467-018-07865-9.
Mudelsee, M., 2003. Estimating Pearson's correlation coefficient with bootstrap confidence interval from serially dependent time series. Math. Geol. 35 (6), 651–665. https://doi.org/10.1023/B:MATG.0000002982.52104.02.
Palmer, J.G., Cook, E.R., Turney, C.S.M., Allen, K.J., Fenwick, P., Cook, B.I., O'Donnell, A., Lough, J., Grierson, P.F., Baker, P., 2015. Drought variability in the eastern Australia and New Zealand summer drought atlas (ANZDA, CE 1500-2012) modulated by the Interdecadal Pacific Oscillation. Environ. Res. Lett. 10 (12). https://doi.org/10.1029/1748-9326/10/12/124002.
Parker, D., Folland, C., Scaife, A., Knight, J., Colman, A., Baines, P., Dong, B., 2007. Decadal to multidecadal variability and the climate change background. J. Geophys. Res. Atmos. 112 (D18). https://doi.org/10.1029/2007jd008411.
Power, S., Casey, T., Folland, C., Colman, A., Mehta, V., 1999. Inter-decadal modulation of the impact of ENSO on Australia. Clim. Dyn. 15 (5), 319–324. https://doi.org/10.1007/s003820050284.
Schneider, D.P., Okumura, Y., Deser, C., 2012. Observed antarctic interannual climate variability and tropical linkages. J. Clim. 25 (12), 4048–4066. https://doi.org/10.1175/jcli-d-11-00273.1.
Sheffield, J., Wood, E.F., Roderick, M.L., 2012. Little change in global drought over the past 60 years. Nature 491, 435–438. https://doi.org/10.1038/nature11575.
Tozer, C.R., Kiem, A.S., Verdon-Kidd, D.C., 2012. On the uncertainties associated with using gridded rainfall data as a proxy for observed. Hydrol. Earth Syst. Sci. 16, 1481–1499. https://doi.org/10.5194/hess-16-1481-2012.
Tozer, C.R., Vance, T.R., Roberts, J.L., Kiem, A.S., Curran, M.A.J., Moy, A.D., 2016. An ice core derived 1013-year catchment-scale annual rainfall reconstruction in subtropical eastern Australia. Hydrol. Earth Syst. Sci. 20, 1703–1717. https://doi.org/10.5194/hess-20-1703-2016.
Turner, J., 2004. The el niño–southern oscillation and Antarctica. Int. J. Climatol. 24 (1), 1–31. https://doi.org/10.1002/joc.965.
van Dijk, A.I.J.M., Beck, H.E., Crosbie, R.S., de Jeu, R.A.M., Liu, Y.Y., Podger, G.M., Timbal, B., Viney, N.R., 2013. The millennium drought in southeast Australia (2001–2009): natural and human causes and implications for water resources, ecosystems, economy and society. Water Resour. Res. 49, 1–18. https://doi.org/10.1002/wrcr.20123.
Van Loon, A.F., 2015. Hydrological drought explained. WIREs Water 2, 359–392. https://doi.org/10.1002/wat2.1085.
van Ommen, T.D., Morgan, V., 2010. Snowfall increase in coastal East Antarctica linked with southwest Western Australian drought. Nat. Geosci. 3 (4), 267–272. https://doi.org/10.1038/ngeo761.
Vance, T.R., Ommen, T.Dv., Curran, M.A.J., Plummer, C.T., Moy, A.D., 2013. A millennial proxy record of ENSO and eastern australian rainfall from the law dome ice core, East Antarctica. J. Clim. 26 (3), 710–725. https://doi.org/10.1175/jcli-d-12-00003.1.
Vance, T.R., Roberts, J.L., Plummer, C.T., Kiem, A.S., van Ommen, T.D., 2015. Interdecadal Pacific variability and eastern Australian mega-droughts over the last millennium. Geophys. Res. Lett. 41. https://doi.org/10.1002/2014GL062447.
Vance, T.R., Roberts, J.L., Moy, A.D., Curran, M.A.J., Tozer, C.R., Gallant, A.J.E., Abram, N.J., van Ommen, T.D., Young, D.A., Grima, C., Blankenship, D.D., Siegert, M.J., 2016. Optimal site selection for a high-resolution ice core record in East Antarctica. Clim. Past 12 (3), 595–610. https://doi.org/10.5194/cp-12-595-2016.
Verdon-Kidd, D.C., Kiem, A.S., 2009. Nature and causes of protracted droughts in Southeast Australia - Comparison between the Federation, WWII and Big Dry droughts. Geophys. Res. Lett. 36, L22707. https://doi.org/10.1029/2009GL041067.
Zhang, L., Kuczera, G., Kiem, A.S., Willgoose, G.R., 2018. Using paleoclimate reconstructions to analyse hydrological epochs associated with Pacific decadal variability. Hydrol. Earth Syst. Sci. 22, 6399–6414. https://doi.org/10.5194/hess-22-6399-2018.